

24 **Abstract**

25 Chagas disease (CD) is a neglected tropical disease caused by the parasitic protozoan
26 *Trypanosoma cruzi*. However, only 20% to 30% of infected individuals will progress to severe
27 symptomatic cardiac manifestations. Current treatments are benznidazole and nifurtimox, which
28 are poorly tolerated regimens. Developing a biomarker to determine the likelihood of patient
29 progression would be helpful for doctors to optimize patient treatment strategies. Such a biomarker
30 would also benefit drug discovery efforts and clinical trials. In this study, we combined untargeted
31 and targeted metabolomics to compare serum samples from *T. cruzi*-infected individuals who
32 progressed to severe cardiac disease, versus infected individuals who remained at the same disease
33 stage (non-progressors). We identified four unannotated biomarker candidates, which were
34 validated in an independent cohort using both untargeted and targeted analysis techniques. Overall,
35 our findings demonstrate that serum small molecules can predict CD progression, offering
36 potential for clinical monitoring.

37

38 **Keywords**

39 Chagas disease; *Trypanosoma cruzi*; disease progression; biomarkers; metabolomics; mass
40 spectrometry

41

42

43 Introduction

44 Chagas disease (CD), caused by *Trypanosoma cruzi* parasites, is a vector-borne illness with
45 a wide geographic range, primarily endemic to rural areas but also found in urban settings across
46 Mexico, Central America, and South America This neglected tropical disease is continually
47 expanding its range and impact due to climate change and migration; with cases found as far as
48 Japan ¹. If untreated, *T. cruzi* infection is lifelong and can be life-threatening. CD can result in
49 various complications, including megaesophagus, megacolon, arrhythmias, apical aneurysms,
50 congestive heart failure, thromboembolism, and sudden death. Among these, Chagas
51 cardiomyopathy is the most severe manifestation of the disease. Up to 30% of chronically infected
52 people develop cardiac complications, while 10% develop digestive, neurological, or mixed
53 symptomatology ².

54 The primary diagnosis method in chronic CD is serology ³. PCR detection can only
55 demonstrate failure to clear parasites, not treatment success, given its high rate of false negatives
56 ⁴⁻⁶. Given these limitations, there have been considerable efforts made to identify alternative
57 markers of successful parasite clearance and/or disease progression. These strategies include
58 detection of antibodies to specific parasite proteins or parasite glycotopes ^{7,8,9,10,11}, host protein
59 fragments ^{12,13}, coagulation factors ¹⁴, or evaluation of immune cell types ^{15,16}. A critical limitation
60 of all these approaches, however, is that they rely on parasite clearance as a measure of treatment
61 success and prognosis. However, the BENEFIT clinical trial demonstrated that, when treatment
62 is administered to patients with pre-existing cardiac abnormalities, parasite clearance is
63 insufficient to prevent disease progression or mortality ¹⁷. Therefore, biomarkers that only measure
64 parasite clearance are insufficient to predict clinical outcomes.

65 Multiple protein biomarkers have been correlated with CD stage, though none yet have
66 proven useful in a clinical context. IFN- γ is essential for the control of *T. cruzi* infection in
67 experimental models. Serum from patients with chronic Chagasic cardiomyopathy had relatively
68 high expression of IFN- γ compared to noncardiac or indeterminate CD patients^{18,19}. A recent study
69 found that differences in the levels of 44 host proteins correlated with clinical progression.
70 Interestingly, while many of those proteins were immune-associated, several of them (ATP5IF1,
71 B4GALT1, GMPR, ISM1, AGRP) were linked to human metabolism²⁰. Other protein biomarkers
72 of CD severity (TNF α , brain natriuretic peptide (BNP), or the MMP-2/MMP-9 ratio, for example),
73 only differentiate between symptomatic and asymptomatic patients or between advanced and early
74 stages of cardiomyopathy, and may not be able to predict disease progression in asymptomatic
75 individuals^{21–24,25}. BNP is a very nonspecific marker of congestive heart failure and is therefore
76 unsuitable as an early biomarker^{26,23}.

77 Serum and urine metabolites have been identified as indicators of *T. cruzi* infection status
78 in human subjects and mouse models^{27,28,29}. The level of cardiac acylcarnitines and
79 glycerophosphocholines were correlated with markers of cardiac inflammation and fibrosis³⁰.
80 Furthermore, the cardiac metabolome could be used to predict infection outcome in acute mouse
81 models of infection³¹. A recent study showed that some metabolites could be restored by treatment
82 with the antiparasitic nifurtimox²⁸. However, studies of metabolites as biomarkers of CD
83 progression are lacking, especially in humans. Therefore, we analyzed samples from a multiyear
84 cohort of *T. cruzi*-infected Bolivians, comparing CD patients who showed cardiac disease
85 progression, to patients who remained asymptomatic, and found four metabolites to be promising
86 biomarker candidates. Two of these metabolites showed increased levels in infected progressors
87 at baseline compared to non progressors, while the other two were decreased in infected

88 progressors.. Given the significant adverse effects of antiparasitic drugs and intermittent drug
89 shortages ³², biomarkers of disease progression could help target more effective screening and
90 interventions towards those who would benefit from them the most.

91

92 **Results**

93 **Study participants**

94 To explore potential metabolite biomarkers of progression to more severe cardiac disease
95 in patients chronically infected with *T. cruzi*, we studied four groups: infected progressors (N=37),
96 infected non-progressors (N=91), uninfected ‘progressors’ (patients with non Chagasic heart
97 failure ; N=3) and uninfected non-progressors (healthy controls; N=13) (see Methods). Infected
98 patients were monitored over 3 years. Patients that showed no symptoms, normal
99 electrocardiogram (EKG) and normal echocardiograms were defined as stage A. Patients who
100 showed no symptoms but had abnormal EKG fitting specific criteria were defined as stage B.
101 Patients showing systolic dysfunction in echocardiogram (EF < 50) were defined as stage C or D.
102 If a patient progressed from stage A to B or B to C/D during the study, they were classified as
103 progressors, while the non-progressors were those that remained at stage A or B. Importantly,
104 samples were collected from progressors prior to disease advancement, so that any metabolic
105 changes identified in this study can serve as prospective biomarkers of disease progression. The
106 uninfected progressors group was used to evaluate whether the observed metabolite changes were
107 specific to chagasic cardiomyopathy or also found in nonchagasic pathologies.

108 We matched patients from the infected progressor group and patients from the infected
109 non-progressor group by gender, initial disease stage and age difference smaller than 5 years (see

110 Methods). Patient serum samples were analyzed by HPLC-MS/MS for untargeted metabolomic
111 analysis as described in the methods section, using two different chromatography methods
112 (pHILIC and polar C18), and MS data acquisition in positive and negative mode. Samples were
113 from two separate shipments of different patients, serving as two separate cohorts.

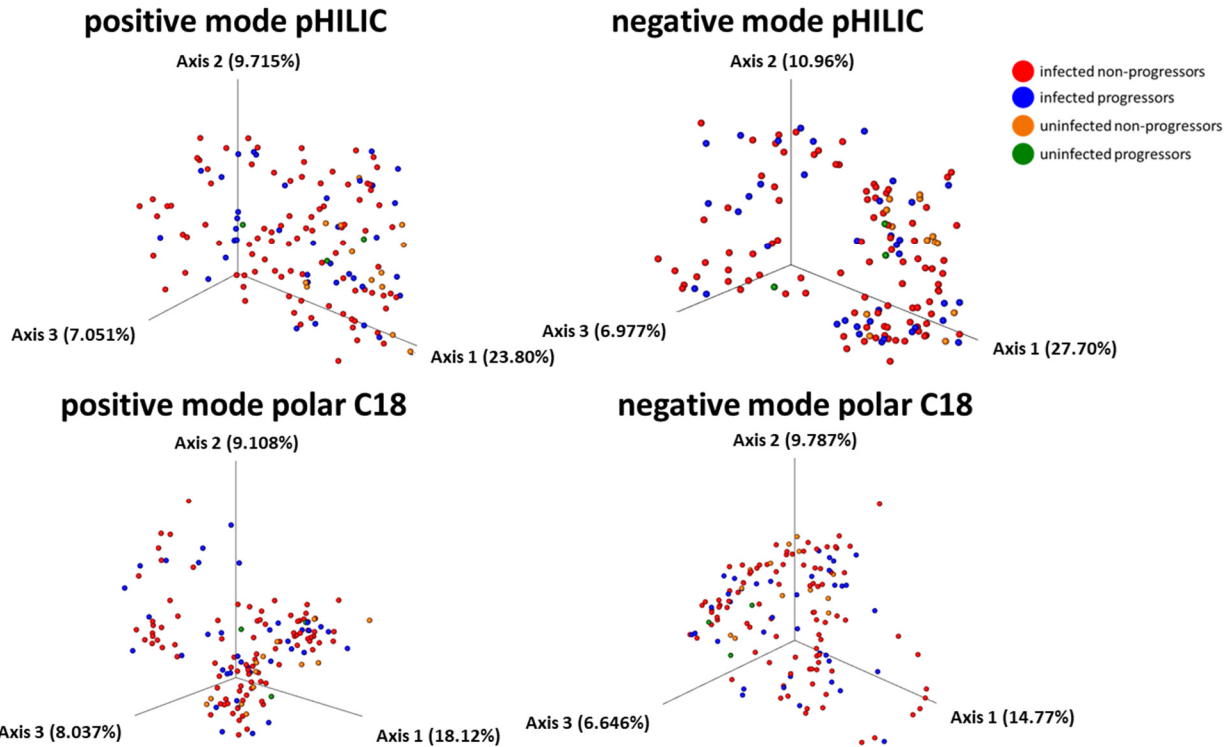
114 **Limited association of progressing vs non-progressing status and overall metabolome**

115 In terms of the overall metabolite profile (both cohorts combined), as shown in **Figure 1**,
116 all four groups clustered with each other. There was no significant difference in overall
117 metabolome between groups in polar C18 datasets, except between infected non-progressors and
118 uninfected non-progressors in positive mode ($p=0.048$ and pseudo- $F=2.128$), reflecting the impact
119 of infection on the metabolome. For pHILIC chromatography in both polarities, there were
120 likewise significant differences in overall metabolome for infected non-progressors vs uninfected
121 non-progressors ($p=0.006$ and pseudo- $F=3.815$ for positive mode, $p=0.012$ and pseudo- $F=3.920$
122 for negative mode), as well as differences between infected progressors vs uninfected non-
123 progressors ($p=0.021$ and pseudo- $F=2.905$ for positive mode, $p=0.042$ and pseudo- $F=2.987$ for
124 negative mode) (**Table 1**).

125

126

127



128

129 **Figure 1. Limited overall differences in serum metabolite profile between uninfected non-**
 130 **progressor group, uninfected progressor group, infected non-progressor group, and infected**
 131 **progressor group from pHILIC and polar C18 separation in both positive mode and negative**
 132 **mode data. All four groups showed overlap.**

133

134 **Table 1. Limited differences in overall metabolism between the four different patient groups.**
 135 **PERMANOVA p values with Benjamini-Hochberg FDR correction. Bold, FDR-corrected p<0.05.**

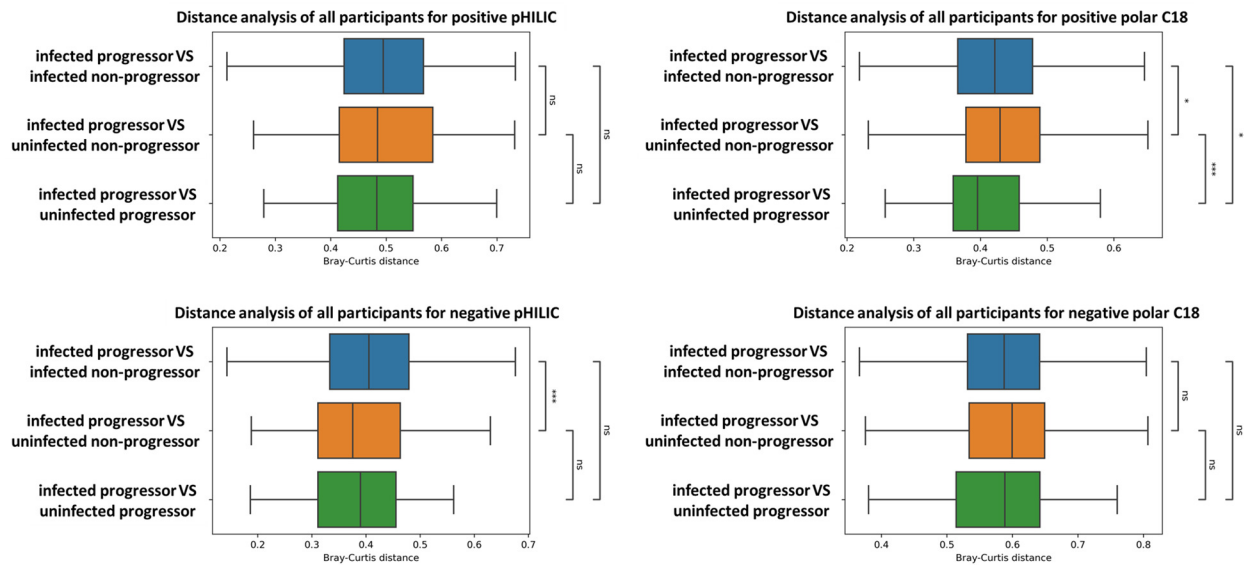
datasets	group 1	group 2	p value	pseudo F
pHILIC in positive mode	infected non-progressors	infected progressors	0.3640	1.330964
	infected non-progressors	uninfected non-progressors	0.0120	3.846872
	infected non-progressors	uninfected progressors	0.8130	0.664337
	infected progressors	uninfected non-progressors	0.0120	2.904537
	infected progressors	uninfected progressors	0.8130	0.685083
	uninfected non-progressors	uninfected progressors	0.6285	1.021994
	infected non-progressors	infected progressors	0.941	0.586750

pHILIC in negative mode	infected non-progressors	uninfected non-progressors	0.018	3.937563
	infected non-progressors	uninfected progressors	0.941	0.590266
	infected progressors	uninfected non-progressors	0.030	2.987234
	infected progressors	uninfected progressors	0.941	0.442172
	uninfected non-progressors	uninfected progressors	0.648	1.113972
polar C18 in positive mode	infected non-progressors	infected progressors	0.526	1.129306
	infected non-progressors	uninfected non-progressors	0.048	2.128310
	infected non-progressors	uninfected progressors	0.931	0.741003
	infected progressors	uninfected non-progressors	0.117	1.707515
	infected progressors	uninfected progressors	0.931	0.642245
	uninfected non-progressors	uninfected progressors	0.931	0.674938
polar C18 in negative mode	infected non-progressors	infected progressors	0.4275	1.170979
	infected non-progressors	uninfected non-progressors	0.3480	1.528665
	infected non-progressors	uninfected progressors	0.4275	1.113128
	infected progressors	uninfected non-progressors	0.3570	1.364624
	infected progressors	uninfected progressors	0.4290	1.012039
	uninfected non-progressors	uninfected progressors	0.4290	1.037428

136

137 Interestingly, for negative mode pHILIC data, infected progressors were more divergent
138 from infected non-progressors than from uninfected non-progressors in terms of overall
139 metabolome. For the positive mode polar C18 dataset, the infected progressors vs uninfected non-
140 progressors showed the largest difference compared to infected progressors vs infected non-

141 progressors and infected progressors vs uninfected progressors in terms of overall metabolome,
142 indicating that infected progressors have a distinct serum metabolite profile compared to infected
143 non-progressors and uninfected non-progressors. The smaller difference between infected
144 progressors and uninfected progressors in terms of overall metabolome suggests that progressed
145 heart disease could show similar predictive metabolite profiles, with the caveat that only few
146 uninfected progressor samples were available in this study. There were no significant differences
147 between inter-group overall metabolic distances in positive mode pHILIC and negative mode polar
148 C18 datasets (**Figure 2**).



149

150 **Figure 2. PCoA distances between different progression groups.** All cohorts, sexes and ages
151 combined. P values are calculated by Mann-Whitney U test, two-sided, FDR-corrected, *: 1.00e-
152 02 < p ≤ 5.00e-02, **: 1.00e-03 < p ≤ 1.00e-02, ***: 1.00e-04 < p ≤ 1.00e-03, ****: p ≤ 1.00e-04.
153 ns, non-significant.

154

155

156 **Limited confounding impact of age and sex**

157 We also assessed whether different sexes showed different metabolite profiles associated
158 with disease progression. However, as shown in **Figure S1**, we found that all four datasets showed
159 no differences in terms of overall metabolome between experimental groups in both male and
160 female subjects.

161 Samples were selected to have equal age representation and sex representation between
162 groups. However, we performed multi-parameter PERMANOVA to test the interaction between
163 age and sex, to know whether sex and age effects reduced our statistical power or masked effects
164 of disease on the metabolites. Positive mode pHILIC and polar C18 datasets showed a significant
165 effect of age but not sex. However, negative mode pHILIC showed a significant effect of sex and
166 age, and negative polar C18 showed no significant effect of sex or age (**Table 2**). Importantly, all
167 four datasets showed no significant interactions between disease progression status and gender or
168 age (**Table 2**, PERMANOVA $p > 0.05$). These results indicate that the different ages of the subjects
169 are impacting the metabolome, but not confounding our interpretation of disease outcomes, so we
170 chose to not subset the dataset by age or sex and analyze all samples jointly.

171

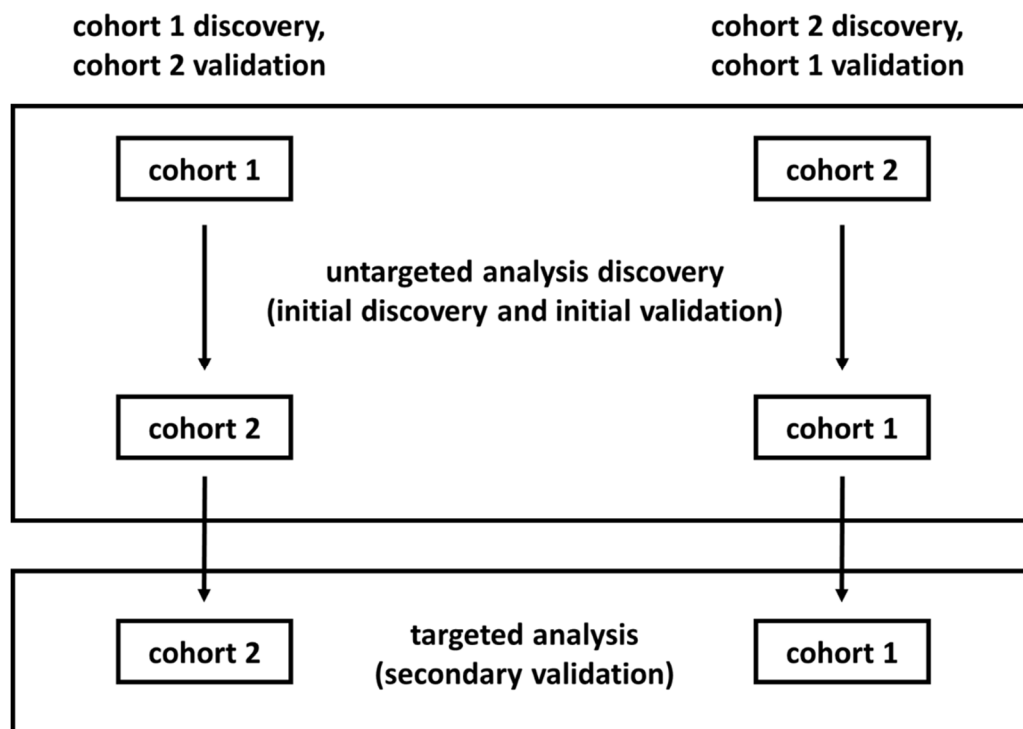
172 **Table 2. p values of multi-parameter PERMANOVA for interaction between gender, age**
173 **and infection status. Bold, p<0.05.**

datasets	statistical results	gender	age	CD status	gender & age	CD status & age	CD status & gender
positive pHILIC	R ²	0.011559	0.016552	0.038838	0.005335	0.016831	0.019426
	p value	0.062	0.017	0.006	0.659	0.792	0.567
negative pHILIC	R ²	0.017923	0.023319	0.033940	0.006735	0.014676	0.012115
	p value	0.012	0.007	0.041	0.375	0.869	0.963
positive polar C18	R ²	0.010340	0.017939	0.026836	0.007124	0.017459	0.017973
	p value	0.075	0.005	0.079	0.378	0.780	0.736
negative polar C18	R ²	0.010930	0.010042	0.026023	0.007260	0.018661	0.018322
	p value	0.055	0.102	0.102	0.375	0.687	0.714

174

175 **Discovery of individual metabolites predictive of progression status**

176 To enable biomarker discovery and validation in separate cohorts, we separated samples
177 based on shipments into two cohorts. Cohort 1 was used to discover candidate biomarkers, with
178 validation in cohort 2, and vice versa, using untargeted metabolomics data to discover candidates,
179 which were subsequently validated by targeted parallel reaction monitoring (PRM) analysis
180 **(Figure 3).**



181

182 **Figure 3. Diagram of the cross-validation between different cohorts.** For cohort 1, N=26
183 infected progressors, N=69 infected non-progressors, N=3 uninfected progressors, N=13
184 uninfected non-progressors. For cohort 2, N=11 infected progressors, N=22 infected non-
185 progressors.
186

187 Our discovery significance cutoff was uncorrected two-sided Mann-Whitney-Wilcoxon
188 $p < 0.05$ for infected progressors vs infected non-progressors. We made this choice to select the
189 broadest range of candidates in the inclusion list for targeted analysis and minimize false negatives.
190 Targeted analysis on the second cohort then serves as independent validation, to eliminate any
191 false positives. We then assessed if metabolites that met this significance criterion showed the
192 same direction of changes in both cohorts, with no significance cutoff. Lastly, we performed ROC
193 analysis, with $AUC > 0.65$ to filter this inclusion list for PRM analysis. However, in positive mode
194 polar C18 cohort 1 discovery analysis, following the AUC cutoff, no candidate remained. To
195 expand the inclusion list for targeted analysis, we therefore manually added four additional specific
196 m/z based on the literature on CD pathogenesis, for evaluation in the validation cohort.

197 Specifically, given our prior findings on impacts of infection on glycerophosphocholines and
 198 purines³³, we manually selected m/z 482.361 (lysophosphocholine O-16:0), m/z 137.046
 199 (hypoxanthine), m/z 348.07 (adenosine diphosphate) and m/z 269.088 (xanthosine) to expand the
 200 inclusion list. We also included these four candidates for validation analysis in cohort 1 (**Table 3**).

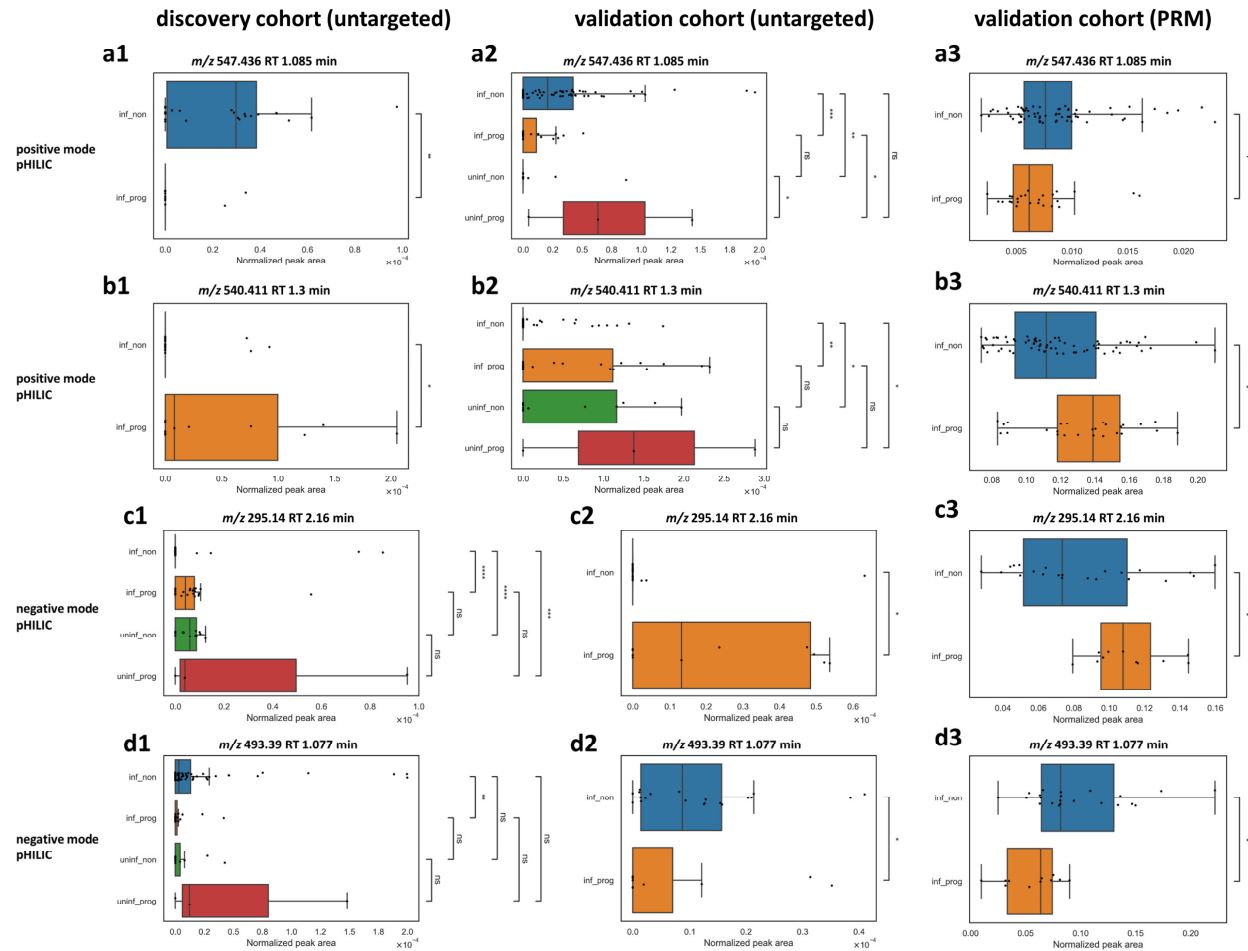
201 Biomarker candidate validation

202 Discovered candidate biomarkers were then validated in the reciprocal patient cohort using
 203 targeted analysis. Using this approach, we validated four biomarker candidates which showed
 204 significant differences between infected progressors and infected non-progressors in the validation
 205 cohort (**Table 3**). Two candidates came from the positive mode pHILIC dataset, and two from the
 206 negative mode pHILIC dataset. As shown in **Figure 4** and **Figure 5**, m/z 547.436 RT (retention
 207 time) 1.085 min from cohort 2 was validated by targeted analysis in cohort 1. m/z 540.411 RT 1.3
 208 min from cohort 2 was validated by targeted analysis in cohort 1. m/z 295.14 RT 2.16 min and
 209 m/z 493.39 RT 1.077 min, from negative mode pHILIC dataset in cohort 1 were validated by
 210 targeted analysis in cohort 2. None of these metabolites had annotations.

211 **Table 3. Candidate metabolite filtering and cross-validation.** * means selection of extra
 212 candidates based on our current knowledge of CD, as described above.

cohort 1 discovery, cohort 2 validation				
	positive pHILIC	negative pHILIC	positive pC18	negative pC18
discovered in cohort 1	308	439	7	11
validated in cohort 2 (untargeted)	3	1	0	1
inclusion list for PRM	3	1	4*	1
PRM validation in cohort 2	0	0	0	0
cohort 2 discovery, cohort 1 validation				
	positive pHILIC	negative pHILIC	positive pC18	negative pC18
discovered in cohort 2	474	410	292	160
validated in cohort 1 (untargeted)	17	13	7	1
inclusion list for PRM	17	13	11*	1
PRM validation in cohort 1	2	2	0	0

213



214

215 **Figure 4. Cross-validated biomarker candidates.** (a) m/z 547.436 RT 1.085 min, from positive
 216 mode pHLIC dataset, initial discovery in cohort 2 (a1) and initial validation in cohort 1 (a2),
 217 secondary validation in cohort 1 (a3). (b) m/z 540.411 RT 1.3 min, from positive mode pHLIC
 218 dataset, initial discovery in cohort 2 (b1) and initial validation in cohort 1 (b2), secondary
 219 validation in cohort 1 (b3). (c) m/z 295.14 RT 2.16 min, from negative mode pHLIC dataset,
 220 initial discovery in cohort 1 (c1) and initial validation in cohort 2 (c2), secondary validation in
 221 cohort 2 (c3). (d) m/z 493.39 RT 1.077 min, from negative mode pHLIC dataset, initial discovery
 222 in cohort 1 (d1) and initial validation in cohort 2 (d2), secondary validation in cohort 2 (d3). All
 223 four metabolites showed significant differences between infected progressors and infected non-
 224 progressors. P values are calculated by Mann-Whitney U test, two-sided, no FDR-correction, *:
 225 $1.00e-02 < p \leq 5.00e-02$, **: $1.00e-03 < p \leq 1.00e-02$, ***: $1.00e-04 < p \leq 1.00e-03$, ****:
 226 $p \leq 1.00e-04$.

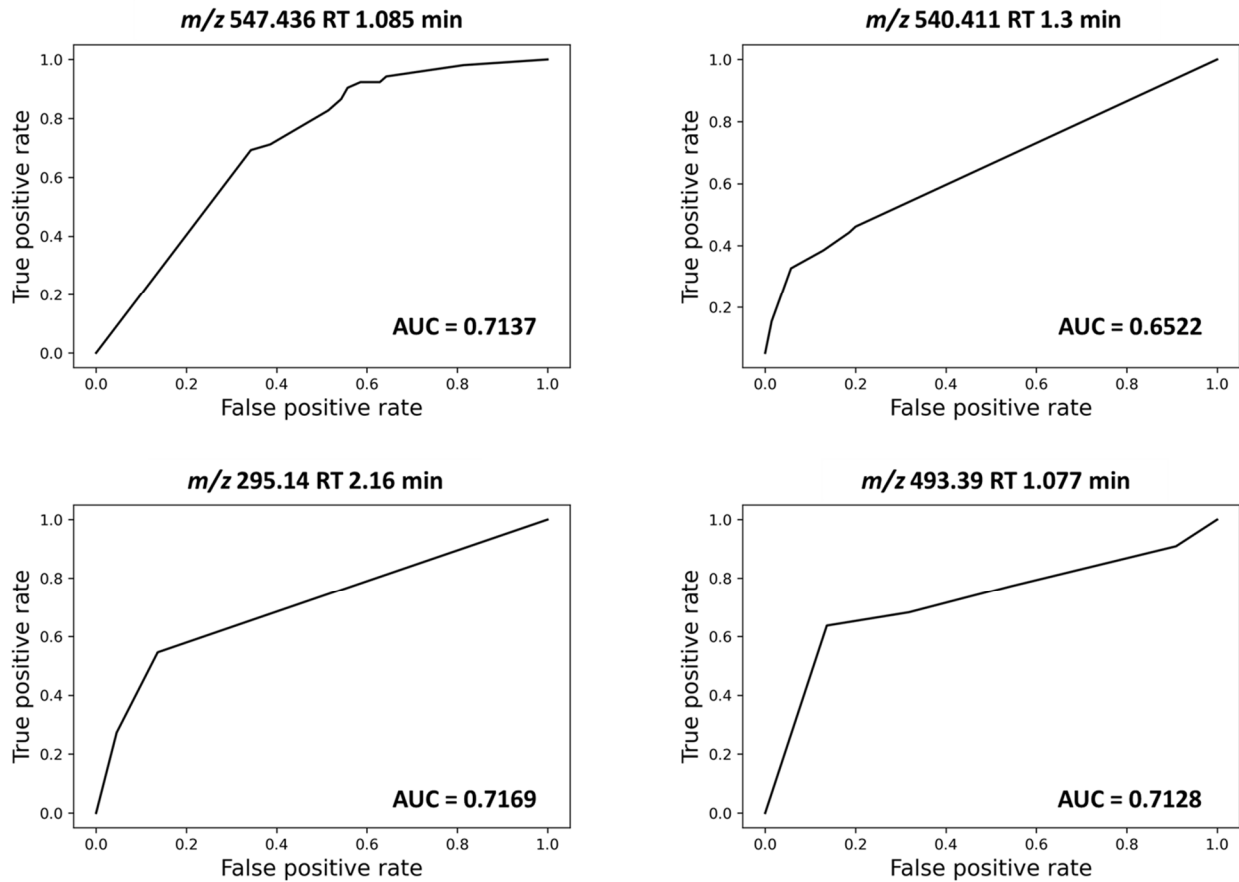
227

228

229

230

231



232

233 **Figure 5. Biomarker ROC curves.** The AUC values for 547.436 RT 1.085 min and m/z 540.411
234 RT 1.3 min came from training in cohort 2 and predicted in cohort 1. The AUC values for m/z
235 295.14 RT 2.16 min and m/z 493.39 RT 1.077 min came from training in cohort 1 and predicted
236 in cohort 2.
237

238 Discussion

239 The ideal biomarker of CD should reflect disease progression, so that doctors can optimize
240 interventions. There is currently no consensus on treatment of asymptomatic adults. Current CDC
241 guidelines recommend treating asymptomatic *T. cruzi*-positive individuals 50 years or younger;
242 treatment is optional for patients over 50 years old due to the high risk of side effects¹⁰. The Pan
243 American Health Organization (PAHO) recommends treatment in asymptomatic patients
244 irrespective of age³⁴, whereas the Brazilian Society of Cardiology sets an age cutoff similar to the

245 CDC³⁵. This age range includes over a quarter of CD patients^{36,37,38} and most of the CD mortality
246³⁹. 14% of adults treated with benznidazole, the preferred agent, will suspend treatment because of
247 adverse effects⁴⁰. A biomarker of disease progression could enable patients to make informed
248 decisions with regards to the relative risks and benefits of treatment, enable assessment of
249 treatment success, or inform clinical trial design.

250 Given prior work showing changes in circulating metabolites with *T. cruzi* infection in
251 mouse models^{29,41}, their association with disease severity in mouse models^{30,42}, and infection-
252 associated metabolite changes in human CD patients²⁸, we hypothesized that metabolite levels in
253 the serum of *T. cruzi*-infected individuals could predict CD progression. Overall metabolite
254 profiles between all four groups (infected progressors, infected non-progressors, uninfected
255 progressors and uninfected non-progressors) were very similar. Given that our discovery analysis
256 was being followed by a validation cohort, we chose to use looser criteria by not using FDR
257 correction for p-values in the discovery cohort. This decision led to low validation rates (**Table 3**),
258 but nevertheless enabled the discovery and validation of four candidate biomarkers at the
259 individual metabolite level. We also chose not to a priori exclude the biomarker candidates that
260 also showed significant differences between uninfected progressor and uninfected non-
261 progressors, because CD can be differentiated from non-CD heart disease through other means
262 (e.g. PCR, serodiagnosis³).

263 One limitation for this project is patient comorbidities and behavioral differences that likely
264 increased variability. Multi-parameter PERMANOVA analysis showed that the different ages of
265 the subjects impact the metabolome, but did not confound our interpretation of disease outcomes
266 (**Table 2**). We therefore elected to analyse all samples jointly, without subsetting the dataset by
267 age or sex and for better statistical power given the limited sample numbers available. Likewise,

268 it is possible that some non-progressors will ultimately progress to symptomatic disease outside
269 this study's follow-up period, in which case our results may be interpreted as differentiating
270 between faster and slower progressors. Even given these limitations, we successfully validated
271 four biomarker candidates. m/z 547.436 RT 1.085 min and m/z 493.39 RT 1.077 min showed
272 decreased levels in infected progressors compared to infected non-progressors, while m/z 540.411
273 RT 1.3 min and m/z 295.14 RT 2.16 min showed increased level in infected progressors compared
274 to infected non-progressors. The lack of annotations for these biomarkers limits the biological
275 insight that can be derived from them. However, from a clinical implementation perspective,
276 annotations are not necessary for disease prediction. To enable cross-study assessment, we provide
277 m/z , retention time and MS/MS spectra, per the recommendations of the Metabolomics Standards
278 Initiative⁴³ (**Table S13**). Given the low parasite burden in chronic CD, these biomarkers are almost
279 certainly of host origin.

280 Further investigation in dogs and other animal models could be implemented to determine
281 whether these biomarkers are common in mammals or only specific to humans. Canine biomarkers
282 would be particularly useful given the high rates of CD in working dogs⁴⁴. Assessment with a
283 larger sample size is necessary for further validation, particularly with regards to patient and
284 parasite genetic diversity. Evaluation of biomarker changes in response to treatment is also
285 necessary.

286 **Conclusion**

287 We have identified four metabolite biomarkers that are predictive of progression to more
288 severe cardiac CD. These biomarkers show promise for use in human cohorts, either in the context

289 of evaluation of new therapeutic modalities, to prioritize treatment when drug availability is
290 limited, or to increase treatment compliance in the highest-risk group.

291

292 **Materials and methods**

293 **Study population**

294 Serum samples were from the Johns Hopkins-Universidad Peruana Cayetano Heredia
295 Collaborated Studies Chagas disease biorepository, Johns Hopkins Institutional Review Board
296 (IRB) approval number IRB00007176. Initial sample collection was under Johns Hopkins
297 Institutional Review Board (IRB) approval number IRB00009799.

298 Samples were collected from Chagas disease patients and uninfected controls at the San
299 Juan de Dios Hospital, Santa Cruz, Bolivia (**Table 4**). As shown in **Table 5**, there were two
300 shipments from the study site, consisting of samples from different study participants. The first
301 shipment included all four groups but the second shipment only contained infected progressors
302 and infected non-progressors. The following staging criteria was used for determination of cardiac
303 progressors vs cardiac non progressors. Advanced stages C and D were determined by ejection
304 fraction (EF) on echocardiography. $40 < EF < 50$ were designated stage C, regardless of EKG
305 results. $EF \leq 40$ was designated stage D, regardless of EKG results. If $EF > 50$, then the EKG results
306 were used to guide staging A vs B. To be classified as stage B, patients must present with at least
307 one of the following conditions: arrhythmias (including Afib/flutter, premature ventricular
308 contractions (PVCs) or ventricular tachycardia), bradycardia (heart rate < 50), blocks (including
309 any AV Block, right bundle branch block, left bundle branch block, left anterior fascicular block,
310 non-specific intraventricular conduction delay, or bi or tri-fascicular blocks), pathologic Q waves,

311 or paced rhythm. A normal EKG or any of the following abnormalities were determined to be stage
 312 A: axis deviation, right ventricular hypertrophy/left ventricular hypertrophy, left atrial
 313 enlargement/right atrial enlargement, low voltage, ST/T alterations, sinus tachycardia, long QT.
 314 These criteria were developed to distinguish EKG changes specifically associated with Chagasic
 315 cardiomyopathy as stage B.

316

317 **Table 4.** Number of subjects with sex and age information.

groups		gender		age			total
		male	female	20-40	40-60	60-80	
uninfected non-progressors	cohort 1	10	3	3	7	3	13
	cohort 2	0	0	0	0	0	0
uninfected progressors	cohort 1	1	2	1	1	1	3
	cohort 2	0	0	0	0	0	0
infected non-progressors	cohort 1	52	17	10	43	16	69
	cohort 2	12	10	1	9	12	22
infected progressors	cohort 1	17	9	2	14	10	26
	cohort 2	6	5	1	4	6	11

318

319 **Table 5.** Number of subjects by disease progression stage.

Groups		stage A	stage B	stage A to B	stage A to C/D	total
uninfected non-progressors	cohort 1	13	0	0	0	13
	cohort 2	0	0	0	0	0
uninfected progressors	cohort 1	0	0	3	0	3
	cohort 2	0	0	0	0	0
infected non-progressors	cohort 1	69	0	0	0	69
	cohort 2	22	0	0	0	22
infected progressors	cohort 1	0	0	25	1	26
	cohort 2	0	0	4	7	11

320

321

322 **Serum sample preparation**

323 Serum metabolites were extracted by adding equal volume of 100% methanol with 0.5 μ M
324 sulfachloropyridazine (Fisher Optima) as internal standard, vortexed for 15 seconds, followed by
325 centrifugation at 14800 RPM for 15 minutes. The supernatant was collected into a 96-well plate,
326 then dried down by a speedvac overnight, as recommended in Dunn et al ⁴⁵. Dried sample plates
327 were stored at -80°C.

328 **Untargeted LC-MS/MS data acquisition**

329 Before LC-MS/MS instrumental analysis, dried extracts were resuspended with 80%
330 acetonitrile (Fisher Optima; LC-MS grade), spiked with 2 μ M sulfadimethoxine (Sigma-Aldrich)
331 as internal standard. Data acquisition was performed under the control of XCalibur and Tune
332 software (ThermoScientific). Five pooled quality controls were injected at run start with injection
333 volume 2 μ L, 3 μ L, 4 μ L, and 5 μ L to ensure system equilibration. Data was then acquired in
334 randomized order, with a blank followed by a pooled quality control every 12 injections. The
335 injection volume for each sample was 5 μ L.

336 A pHILIC LC column (SeQuant® ZIC®-pHILIC, 5 μ m polymer, 150 x 2.1 mm) was used,
337 and the column was kept at 40°C during the run. Liquid chromatography was performed at 0.25
338 mL/min flow rate for 18 min. LC gradient was as follows, with mobile phase A (water with 20
339 mM ammonium acetate pH 9.4) and mobile phase B (acetonitrile): 0-10 min=90% B; 10-12
340 min=decrease to 30% B; 12-12.666 min=hold at 30% B; 12.666-18 min=increase to 90% B.

341 After the pHILIC LC-MS run, sample plates were dried down and resuspended with 100%
342 water (Fisher Optima; LC-MS grade), spiked with 2 μ M sulfadimethoxine (Sigma-Aldrich) as
343 internal standard. A Kinetex polar C18 LC column (Phenomenex; 50 \times 2.1 mm, 1.7 μ m particle

344 size, 100 Å pore size) was used, and the column was kept at 40°C during the run. Liquid
345 chromatography was performed at 0.5 mL/min flow rate for 12.5 min. LC gradient was as follows,
346 with mobile phase A (water + 0.1% formic acid) and mobile phase B (acetonitrile +0.1% formic
347 acid): 0-1 min=5% B; 1-9 min=increase to 100% B; 9-11 min=hold at 100% B; 11-11.5=decrease
348 to 5% B; and 11.5-12.5=5% B. Mass spectrometry data acquisition parameters were the same as
349 pHILIC LC-MS run. In all cases, mass spectrometry data acquisition parameters were as
350 previously published³³.

351 **Targeted LC-MS/MS data acquisition**

352 Resuspension procedure and LC columns were the same as for untargeted LC-MS/MS data
353 acquisition, but mass spectrometry data acquisition was performed in parallel reaction monitoring
354 (PRM) mode. Instrument parameters were the same as for untargeted LC-MS data acquisition.
355 Inclusion lists are in **Tables S5-12**.

356 **Data analysis**

357 For untargeted analysis, collected data were analyzed through MZmine (version 2.53)⁴⁶
358 with parameters as in **Table S14**. Data were filtered to retain features that were present in at least
359 two samples and had MS2 spectra to enable annotation. Blank removal was performed with a
360 minimum threefold difference between the blank and serum samples required for a feature to be
361 retained. Total ion current (TIC) normalization to a constant sum of 1 was performed in Jupyter
362 Notebook using R (version 3.6.1). MZmine output files were uploaded and analyzed by Feature-
363 based molecular networking⁴⁷ in GNPS for annotation³³. Annotations were retrieved using a script
364 developed in our laboratory⁴⁸. Lipid annotations such as glycerophosphocholines,
365 glycerophosphoethanolamines and acylcarnitines were further confirmed by searching the LIPID
366 MAPS Structure Database (LMSD and COMPDB)^{49,50}. Feature tables combined with metadata

367 were analyzed in QIIME2⁵¹ for PCoA plot and distance analysis. Distances were compared using
368 Mann-Whitney-Wilcoxon test two-sided, FDR-corrected. PCoA plots were visualized in
369 EMPeror⁵². For further analysis, feature tables were filtered by the mass list which showed
370 significance between the infected progressed group vs infected non-progressed group. Jupyter
371 Notebook with Python (version 3.8.13) and R (version 3.6.1) were used for statistical analysis and
372 visualization.

373 To identify candidate biomarkers, we used Mann-Whitney-Wilcoxon test two-sided
374 without correction between infected progressors and infected non-progressors. This analysis
375 workflow minimizes false negatives. False positives are eliminated by analysis of an independent
376 set of patients, in the targeted PRM analysis workflow (see below). Fold changes were calculated
377 to confirm that the direction of changes between infected progressors and infected non-progressors
378 were consistent between the two cohorts. We use ROC analysis and an AUC cutoff of 0.65 to
379 further evaluate the performance of the candidate biomarkers between infected progressors and
380 infected non-progressors in the different cohorts. ROC curves were created using scikit-learn
381 (version 1.3.0).

382 For PRM data analysis, collected data from the validation cohorts were analyzed through
383 Skyline software (version 23.1) with parameters as in ²⁷. The exported peak areas were normalized
384 by the peak area of the internal standard (m/z 311.0801 for positive mode and m/z 309.0656 for
385 negative mode). Boxplot visualizations were made in Jupyter Notebook with Python (version
386 3.8.13) and R (version 3.6.1).

387

388 **Data availability**

389 The untargeted MS data generated in this study have been deposited in the MassIVE
390 database for positive mode pHILIC: (MSV000092754),
391 negative mode pHILIC (MSV000092756), positive mode polar C18 (MSV000092757), and
392 negative mode polar C18 (MSV000092758). Feature-based molecular networking for untargeted
393 MS data can be accessed at:
394 <https://gnps.ucsd.edu/ProteoSAFe/status.jsp?task=ad84b5b572864898a733f159320bbd12>
395 (positive mode pHILIC),
396 <https://gnps.ucsd.edu/ProteoSAFe/status.jsp?task=7c725bc5bd23485dad48f5e3d6a5a84a>
397 (negative mode pHILIC),
398 <https://gnps.ucsd.edu/ProteoSAFe/status.jsp?task=73c7f72874d64fe78c9f97657df45bee>
399 (positive mode polar C18),
400 <https://gnps.ucsd.edu/ProteoSAFe/status.jsp?task=1e4c73cec97a4f09bbbd126da52a7262>
401 (negative mode polar C18). The targeted MS data for PRM validation have been deposited in the
402 MassIVE database for positive mode pHILIC (MSV000093740), negative mode pHILIC
403 (MSV000093741), positive mode polar C18: (MSV000093742), and negative mode polar C18
404 (MSV000093743). Representative code has been deposited on GitHub, at
405 <https://github.com/zyliu-OU/McCall-Lab/tree/main/05092023>.
406

407 **Author Contributions**

408 L-I.M. designed the project. Z.L. performed metabolite extraction, LC-MS data
409 acquisition and LC-MS data analysis. Z.L. drafted the initial manuscript, which was edited by L-
410 I.M. with input from all authors. R.H.G. is the PI for the ongoing Bolivian cohort study which
411 provided the samples. R.H.G. and N.M.B. participated in study design, data interpretation, and
412 manuscript editing. K.D. and S.V. performed data management, cleaning, and staging for the
413 samples. G.D.S., M.V., P.C.J., B.M.S., F.T., E.M. and R.M. collected samples and patient data.

414 **Conflicts of interest**

415 The authors have no conflict of interest to declare.

416 **Supporting Information**

417 Figure S1. PCoA distances between different progression groups for male and female
418 participants. Table S1-S4. Annotation of differential metabolites. Table S5-S12. Skyline transition
419 lists. Table S13. MS2 spectra information for cross-validated biomarker candidates. Table S14.
420 MZmine data processing parameters table for all four datasets.

421 **Acknowledgments**

422 This project was supported by NIH award number R21AI156669. Samples were from the
423 Johns Hopkins-Universidad Peruana Cayetano Heredia Collaborated Studies Chagas disease
424 biorepository, with prior sample collection, clinical data collection and some salary support to
425 R.H.G and N.M.B. supported by NIH award number R01AI107028. The content is solely the

426 responsibility of the authors and does not necessarily represent the official views of the National
427 Institutes of Health.

428 **Abbreviations used**

429 CD, Chagas disease;
430 HILIC, Hydrophilic interaction chromatography;
431 LC-MS/MS, liquid chromatography-tandem mass spectrometry;
432 PRM, parallel reaction monitoring;
433 RT, retention time

434

435 **References**

- 436 (1) Moncayo, A. Chagas Disease: Current Epidemiological Trends after the Interruption of
437 Vectors and Transfusional Transmission in the Southern Cone Countries. *Mem. Inst.*
438 *Oswaldo Cruz* **2003**, *98* (5), 577–591.
- 439 (2) Pinazo, M.-J.; Thomas, M.-C.; Bustamante, J.; Almeida, I. C. de; Lopez, M.-C.; Gascon, J.
440 Biomarkers of Therapeutic Responses in Chronic Chagas Disease: State of the Art and
441 Future Perspectives. *Mem. Inst. Oswaldo Cruz* **2015**, *110* (3), 422–432.
- 442 (3) The Use of IgG Antibodies in Conventional and Non-Conventional Immunodiagnostic
443 Tests for Early Prognosis after Treatment of Chagas Disease. *J. Immunol. Methods* **2011**,
444 *370* (1-2), 24–34.
- 445 (4) Russomando, G.; Almirón, M.; Candia, N.; Franco, L.; Sánchez, Z.; de Guillen, I.
446 [Implementation and Evaluation of a Locally Sustainable System of Prenatal Diagnosis to
447 Detect Cases of Congenital Chagas Disease in Endemic Areas of Paraguay]. *Rev. Soc. Bras.*

- 448 *Med. Trop.* **2005**, 38 Suppl 2, 49–54.
- 449 (5) Mora, M. C.; Negrette, O. S.; Marco, D.; Barrio, A.; Ciaccio, M.; Segura, M. A.;
- 450 Basombrío, M. A. EARLY DIAGNOSIS OF CONGENITAL TRYPANOSOMA CRUZI
- 451 INFECTION USING PCR, HEMOCULTURE, AND CAPILLARY CONCENTRATION,
- 452 AS COMPARED WITH DELAYED SEROLOGY. *J. Parasitol.* **2005**, 91 (6), 1468–1473.
- 453 (6) Diez, C. N.; Manattini, S.; Zanuttini, J. C.; Bottasso, O.; Marcipar, I. The Value of
- 454 Molecular Studies for the Diagnosis of Congenital Chagas Disease in Northeastern
- 455 Argentina. *Am. J. Trop. Med. Hyg.* **2008**, 78 (4).
- 456 (7) Krautz, G. M.; Galvão, L. M.; Cançado, J. R.; Guevara-Espinoza, A.; Ouaiissi, A.; Krettli,
- 457 A. U. Use of a 24-Kilodalton Trypanosoma Cruzi Recombinant Protein to Monitor Cure of
- 458 Human Chagas' Disease. *J. Clin. Microbiol.* **1995**. [https://doi.org/10.1128/jcm.33.8.2086-](https://doi.org/10.1128/jcm.33.8.2086-2090.1995)
- 459 [2090.1995](https://doi.org/10.1128/jcm.33.8.2086-2090.1995).
- 460 (8) Meira, W. S. F.; Galvão, L. M. C.; Gontijo, E. D.; Machado-Coelho, G. L. L.; Norris, K. A.;
- 461 Chiari, E. Use of the Trypanosoma Cruzi Recombinant Complement Regulatory Protein To
- 462 Evaluate Therapeutic Efficacy Following Treatment of Chronic Chagasic Patients. *J. Clin.*
- 463 *Microbiol.* **2004**. <https://doi.org/10.1128/jcm.42.2.707-712.2004>.
- 464 (9) Fernández-Villegas, A.; Pinazo, M. J.; Marañón, C.; Thomas, M. C.; Posada, E.; Carrilero,
- 465 B.; Segovia, M.; Gascon, J.; López, M. C. Short-Term Follow-up of Chagasic Patients after
- 466 Benznidazole Treatment Using Multiple Serological Markers. *BMC Infect. Dis.* **2011**, 11
- 467 (1), 1–7.
- 468 (10) Montoya, A. L.; Carvajal, E. G.; Ortega-Rodriguez, U.; Estevao, I. L.; Ashmus, R. A.;
- 469 Jankuru, S. R.; Portillo, S.; Ellis, C. C.; Knight, C. D.; Alonso-Padilla, J.; Izquierdo, L.;
- 470 Pinazo, M.-J.; Gascon, J.; Suarez, V.; Watts, D. M.; Malo, I. R.; Ramsey, J. M.; Alarcón De

- 471 Noya, B.; Noya, O.; Almeida, I. C.; Michael, K. A Branched and Double Alpha-Gal-
472 Bearing Synthetic Neoglycoprotein as a Biomarker for Chagas Disease. *Molecules* **2022**, *27*
473 (17). <https://doi.org/10.3390/molecules27175714>.
- 474 (11) Montoya, A. L.; Gil, E. R.; Heydemann, E. L.; Estevao, I. L.; Luna, B. E.; Ellis, C. C.;
475 Jankuru, S. R.; Alarcón de Noya, B.; Noya, O.; Zago, M. P.; Almeida, I. C.; Michael, K.
476 Specific Recognition of β -Galactofuranose-Containing Glycans of Synthetic
477 Neoglycoproteins by Sera of Chronic Chagas Disease Patients. *Molecules* **2022**, *27* (2).
478 <https://doi.org/10.3390/molecules27020411>.
- 479 (12) Santamaria, C.; Chatelain, E.; Jackson, Y.; Miao, Q.; Ward, B. J.; Chappuis, F.; Ndao, M.
480 Serum Biomarkers Predictive of Cure in Chagas Disease Patients after Nifurtimox
481 Treatment. *BMC Infect. Dis.* **2014**, *14* (1), 1–12.
- 482 (13) Ruiz-Lancheros, E.; Rasoolizadeh, A.; Chatelain, E.; Garcia-Bournissen, F.; Moroni, S.;
483 Moscatelli, G.; Altchek, J.; Ndao, M. Validation of Apolipoprotein A-1 and Fibronectin
484 Fragments as Markers of Parasitological Cure for Congenital Chagas Disease in Children
485 Treated With Benznidazole. *Open Forum Infect Dis* **2018**, *5* (11), ofy236.
- 486 (14) Pinazo, M.-J.; Posada, E. de J.; Izquierdo, L.; Tassies, D.; Marques, A.-F.; de Lazzari, E.;
487 Aldasoro, E.; Muñoz, J.; Abras, A.; Tebar, S.; Gallego, M.; de Almeida, I. C.; Reverter, J.-
488 C.; Gascon, J. Altered Hypercoagulability Factors in Patients with Chronic Chagas Disease:
489 Potential Biomarkers of Therapeutic Response. *PLoS Negl. Trop. Dis.* **2016**, *10* (1),
490 e0004269.
- 491 (15) Bustamante, J. M.; Bixby, L. M.; Tarleton, R. L. Drug-Induced Cure Drives Conversion to a
492 Stable and Protective CD8⁺ T Central Memory Response in Chronic Chagas Disease. *Nat.*
493 *Med.* **2008**, *14* (5), 542–550.

- 494 (16) Cesar, G.; Natale, M. A.; Albareda, M. C.; Alvarez, M. G.; Lococo, B.; De Rissio, A. M.;
495 Fernandez, M.; Castro Eiro, M. D.; Bertocchi, G.; White, B. E.; Zabaleta, F.; Viotti, R.;
496 Tarleton, R. L.; Laucella, S. A. B-Cell Responses in Chronic Chagas Disease: Waning of
497 Trypanosoma Cruzi-Specific Antibody-Secreting Cells Following Successful Etiological
498 Treatment. *J. Infect. Dis.* **2023**, *227* (11), 1322–1332.
- 499 (17) Morillo, C. A.; Marin-Neto, J. A.; Avezum, A.; Sosa-Estani, S.; Rassi, A., Jr; Rosas, F.;
500 Villena, E.; Quiroz, R.; Bonilla, R.; Britto, C.; Guhl, F.; Velazquez, E.; Bonilla, L.; Meeks,
501 B.; Rao-Melacini, P.; Pogue, J.; Mattos, A.; Lazdins, J.; Rassi, A.; Connolly, S. J.; Yusuf,
502 S.; BENEFIT Investigators. Randomized Trial of Benznidazole for Chronic Chagas'
503 Cardiomyopathy. *N. Engl. J. Med.* **2015**, *373* (14), 1295–1306.
- 504 (18) Poveda, C.; Fresno, M.; Gironès, N.; Martins-Filho, O. A.; Ramírez, J. D.; Santi-Rocca, J.;
505 Marin-Neto, J. A.; Morillo, C. A.; Rosas, F.; Guhl, F. Cytokine Profiling in Chagas Disease:
506 Towards Understanding the Association with Infecting Trypanosoma Cruzi Discrete Typing
507 Units (A BENEFIT TRIAL Sub-Study). *PLoS One* **2014**, *9* (3), e91154.
- 508 (19) Sousa, G. R.; Gomes, J. A. S.; Fares, R. C. G.; Damásio, M. P. de S.; Chaves, A. T.;
509 Ferreira, K. S.; Nunes, M. C. P.; Medeiros, N. I.; Valente, V. A. A.; Corrêa-Oliveira, R.;
510 Rocha, M. O. da C. Plasma Cytokine Expression Is Associated with Cardiac Morbidity in
511 Chagas Disease. *PLoS One* **2014**, *9* (3), e87082.
- 512 (20) Sunderraj, A.; Cunha, L. M.; Avila, M.; Alexandria, S.; Ferreira, A. M.; de Oliveira-da
513 Silva, L. C.; Ribeiro, A. L. P.; Nunes, M. do C. P.; Sabino, E. C.; Landay, A.; Kalil, J.;
514 Chevillard, C.; Cunha-Neto, E.; Feinstein, M. J. Parasite DNA and Markers of Decreased
515 Immune Activation Associate Prospectively with Cardiac Functional Decline over 10 Years
516 among Trypanosoma Cruzi Seropositive Individuals in Brazil. *Int. J. Mol. Sci.* **2023**, *25* (1),

- 517 44.
- 518 (21) Ferreira, R. C.; Ianni, B. M.; Abel, L. C. J.; Buck, P.; Mady, C.; Kalil, J.; Cunha-Neto, E.
519 Increased Plasma Levels of Tumor Necrosis Factor-Alpha in
520 Asymptomatic/“indeterminate” and Chagas Disease Cardiomyopathy Patients. *Mem. Inst.*
521 *Oswaldo Cruz* **2003**, *98* (3), 407–411.
- 522 (22) Lima-Costa, M. F.; Cesar, C. C.; Peixoto, S. V.; Ribeiro, A. L. P. Plasma B-Type
523 Natriuretic Peptide as a Predictor of Mortality in Community-Dwelling Older Adults with
524 Chagas Disease: 10-Year Follow-up of the Bambui Cohort Study of Aging. *Am. J.*
525 *Epidemiol.* **2010**, *172* (2), 190–196.
- 526 (23) Okamoto, E. E.; Sherbuk, J. E.; Clark, E. H.; Marks, M. A.; Gandarilla, O.; Galdos-
527 Cardenas, G.; Vasquez-Villar, A.; Choi, J.; Crawford, T. C.; Do, R. Q.; Fernandez, A. B.;
528 Colanzi, R.; Flores-Franco, J. L.; Gilman, R. H.; Bern, C.; Chagas Disease Working Group
529 in Bolivia and Peru. Biomarkers in Trypanosoma Cruzi-Infected and Uninfected Individuals
530 with Varying Severity of Cardiomyopathy in Santa Cruz, Bolivia. *PLoS Negl. Trop. Dis.*
531 **2014**, *8* (10), e3227.
- 532 (24) Clark, E. H.; Marks, M. A.; Gilman, R. H.; Fernandez, A. B.; Crawford, T. C.; Samuels, A.
533 M.; Hidron, A. I.; Galdos-Cardenas, G.; Menacho-Mendez, G. S.; Bozo-Gutierrez, R. W.;
534 Martin, D. L.; Bern, C. Circulating Serum Markers and QRS Scar Score in Chagas
535 Cardiomyopathy. *Am. J. Trop. Med. Hyg.* **2015**, *92* (1), 39–44.
- 536 (25) Sherbuk, J. E.; Okamoto, E. E.; Marks, M. A.; Fortuny, E.; Clark, E. H.; Galdos-Cardenas,
537 G.; Vasquez-Villar, A.; Fernandez, A. B.; Crawford, T. C.; Do, R. Q.; Flores-Franco, J. L.;
538 Colanzi, R.; Gilman, R. H.; Bern, C. Biomarkers and Mortality in Severe Chagas
539 Cardiomyopathy. *Glob. Heart* **2015**, *10* (3), 173–180.

- 540 (26) Weber, M.; Hamm, C. Role of B-Type Natriuretic Peptide (BNP) and NT-proBNP in
541 Clinical Routine. *Heart* **2006**, *92* (6), 843–849.
- 542 (27) Dean, D. A.; Roach, J.; vonBargen, R. U.; Xiong, Y.; Kane, S. S.; Klechka, L.; Wheeler, K.;
543 Sandoval, M. J.; Lesani, M.; Hossain, E.; Katemauswa, M.; Schaefer, M.; Harris, M.;
544 Barron, S.; Liu, Z.; Pan, C.; McCall, L.-I. Persistent Biofluid Small-Molecule Alterations
545 Induced by Trypanosoma Cruzi Infection Are Not Restored by Parasite Elimination. *ACS*
546 *Infectious Diseases* **2023**. <https://doi.org/10.1021/acsinfecdis.3c00261>.
- 547 (28) Golizeh, M.; Nam, J.; Chatelain, E.; Jackson, Y.; Ohlund, L. B.; Rasoolizadeh, A.;
548 Camargo, F. V.; Mahrouche, L.; Furtos, A.; Sleno, L.; Ndao, M. New Metabolic Signature
549 for Chagas Disease Reveals Sex Steroid Perturbation in Humans and Mice. *SSRN*
550 *Electronic Journal*. <https://doi.org/10.2139/ssrn.4050413>.
- 551 (29) Lizardo, K.; Ayyappan, J. P.; Ganapathi, U.; Dutra, W. O.; Qiu, Y.; Weiss, L. M.;
552 Nagajyothi, J. F. Diet Alters Serum Metabolomic Profiling in the Mouse Model of Chronic
553 Chagas Cardiomyopathy. *Dis. Markers* **2019**, *2019*, 4956016.
- 554 (30) Hoffman, K.; Liu, Z.; Hossain, E.; Bottazzi, M. E.; Hotez, P. J.; Jones, K. M.; McCall, L.-I.
555 Alterations to the Cardiac Metabolome Induced by Chronic Infection Relate to the Degree
556 of Cardiac Pathology. *ACS Infect Dis* **2021**, *7* (6), 1638–1649.
- 557 (31) McCall, L.-I.; Morton, J. T.; Bernatchez, J. A.; de Siqueira-Neto, J. L.; Knight, R.;
558 Dorrestein, P. C.; McKerrow, J. H. Mass Spectrometry-Based Chemical Cartography of a
559 Cardiac Parasitic Infection. *Anal. Chem.* **2017**, *89* (19), 10414–10421.
- 560 (32) Viotti, R.; Vigliano, C.; Lococo, B.; Alvarez, M. G.; Petti, M.; Bertocchi, G.; Armenti, A.
561 Side Effects of Benznidazole as Treatment in Chronic Chagas Disease: Fears and Realities.
562 *Expert Rev. Anti. Infect. Ther.* **2009**, *7* (2), 157–163.

- 563 (33) Liu, Z.; Ulrich vonBargen, R.; Kendricks, A. L.; Wheeler, K.; Leão, A. C.;
- 564 Sankaranarayanan, K.; Dean, D. A.; Kane, S. S.; Hossain, E.; Pollet, J.; Bottazzi, M. E.;
- 565 Hotez, P. J.; Jones, K. M.; McCall, L.-I. Localized Cardiac Small Molecule Trajectories and
- 566 Persistent Chemical Sequelae in Experimental Chagas Disease. *Nat. Commun.* **2023**, *14* (1),
- 567 1–22.
- 568 (34) Organización Panamericana de la Salud. [Synthesis of evidence: Guidance for the diagnosis
- 569 and treatment of Chagas diseaseSíntese de evidências: Guia de diagnóstico e tratamento da
- 570 doença de Chagas]. *Rev. Panam. Salud Publica* **2020**, *44*, e28.
- 571 (35) Marin-Neto, J. A.; Rassi, A., Jr; Oliveira, G. M. M.; Correia, L. C. L.; Ramos Júnior, A. N.;
- 572 Luquetti, A. O.; Hasslocher-Moreno, A. M.; Sousa, A. S. de; Paola, A. A. V. de; Sousa, A.
- 573 C. S.; Ribeiro, A. L. P.; Correia Filho, D.; Souza, D. do S. M. de; Cunha-Neto, E.; Ramires,
- 574 F. J. A.; Bacal, F.; Nunes, M. do C. P.; Martinelli Filho, M.; Scanavacca, M. I.; Saraiva, R.
- 575 M.; Oliveira Júnior, W. A. de; Lorga-Filho, A. M.; Guimarães, A. de J. B. de A.; Braga, A.
- 576 L. L.; Oliveira, A. S. de; Sarabanda, A. V. L.; Pinto, A. Y. das N.; Carmo, A. A. L. do;
- 577 Schmidt, A.; Costa, A. R. da; Ianni, B. M.; Markman Filho, B.; Rochitte, C. E.; Macêdo, C.
- 578 T.; Mady, C.; Chevillard, C.; Virgens, C. M. B. das; Castro, C. N. de; Britto, C. F. D. P. de
- 579 C.; Pisani, C.; Rassi, D. do C.; Sobral Filho, D. C.; Almeida, D. R. de; Bocchi, E. A.;
- 580 Mesquita, E. T.; Mendes, F. de S. N. S.; Gondim, F. T. P.; Silva, G. M. S. da; Peixoto, G. de
- 581 L.; Lima, G. G. de; Veloso, H. H.; Moreira, H. T.; Lopes, H. B.; Pinto, I. M. F.; Ferreira, J.
- 582 M. B. B.; Nunes, J. P. S.; Barreto-Filho, J. A. S.; Saraiva, J. F. K.; Lannes-Vieira, J.;
- 583 Oliveira, J. L. M.; Armaganijan, L. V.; Martins, L. C.; Sangenis, L. H. C.; Barbosa, M. P.
- 584 T.; Almeida-Santos, M. A.; Simões, M. V.; Yasuda, M. A. S.; Moreira, M. da C. V.;
- 585 Higuchi, M. de L.; Monteiro, M. R. de C. C.; Mediano, M. F. F.; Lima, M. M.; Oliveira, M.

- 586 T. de; Romano, M. M. D.; Araujo, N. N. S. L. de; Medeiros, P. de T. J.; Alves, R. V.;
- 587 Teixeira, R. A.; Pedrosa, R. C.; Aras Junior, R.; Torres, R. M.; Povia, R. M. D. S.; Rassi, S.
- 588 G.; Alves, S. M. M.; Tavares, S. B. do N.; Palmeira, S. L.; Silva Júnior, T. L. da; Rodrigues,
- 589 T. da R.; Madrini Junior, V.; Brant, V. M. da C.; Dutra, W. O.; Dias, J. C. P. SBC Guideline
- 590 on the Diagnosis and Treatment of Patients with Cardiomyopathy of Chagas Disease - 2023.
- 591 *Arq. Bras. Cardiol.* **2023**, *120* (6), e20230269.
- 592 (36) Herrador, Z.; Rivas, E.; Gherasim, A.; Gomez-Barroso, D.; García, J.; Benito, A.; Aparicio,
- 593 P. Using Hospital Discharge Database to Characterize Chagas Disease Evolution in Spain:
- 594 There Is a Need for a Systematic Approach towards Disease Detection and Control. *PLoS*
- 595 *Negl. Trop. Dis.* **2015**, *9* (4), e0003710.
- 596 (37) de Oliveira-Marques, D. S.; Bonametti, A. M.; Matsuo, T.; Gregori Junior, F. The
- 597 Epidemiologic Profile and Prevalence of Cardiopathy in Trypanosoma Cruzi Infected Blood
- 598 Donor Candidates, Londrina, Paraná, Brazil. *Rev. Inst. Med. Trop. Sao Paulo* **2005**, *47* (6),
- 599 321–326.
- 600 (38) Meymandi, S. K.; Forsyth, C. J.; Soverow, J.; Hernandez, S.; Sanchez, D.; Montgomery, S.
- 601 P.; Traina, M. Prevalence of Chagas Disease in the Latin American-Born Population of Los
- 602 Angeles. *Clin. Infect. Dis.* **2017**, *64* (9), 1182–1188.
- 603 (39) Herricks, J. R.; Hotez, P. J.; Wanga, V.; Coffeng, L. E.; Haagsma, J. A.; Basáñez, M.-G.;
- 604 Buckle, G.; Budke, C. M.; Carabin, H.; Fèvre, E. M.; Fürst, T.; Halasa, Y. A.; King, C. H.;
- 605 Murdoch, M. E.; Ramaiah, K. D.; Shepard, D. S.; Stolk, W. A.; Undurraga, E. A.;
- 606 Stanaway, J. D.; Naghavi, M.; Murray, C. J. L. The Global Burden of Disease Study 2013:
- 607 What Does It Mean for the NTDs? *PLoS Negl. Trop. Dis.* **2017**, *11* (8), e0005424.
- 608 (40) Crespillo-Andújar, C.; Venanzi-Rullo, E.; López-Vélez, R.; Monge-Maillo, B.; Norman, F.;

- 609 López-Polín, A.; Pérez-Molina, J. A. Safety Profile of Benznidazole in the Treatment of
610 Chronic Chagas Disease: Experience of a Referral Centre and Systematic Literature Review
611 with Meta-Analysis. *Drug Saf.* **2018**, *41* (11), 1035–1048.
- 612 (41) Gironès, N.; Carbajosa, S.; Guerrero, N. A.; Poveda, C.; Chillón-Marinas, C.; Fresno, M.
613 Global Metabolomic Profiling of Acute Myocarditis Caused by *Trypanosoma Cruzi*
614 Infection. *PLoS Negl. Trop. Dis.* **2014**, *8* (11), e3337.
- 615 (42) Hossain, E.; Khanam, S.; Dean, D. A.; Wu, C.; Lostracco-Johnson, S.; Thomas, D.; Kane,
616 S. S.; Parab, A. R.; Flores, K.; Katemauswa, M.; Gosmanov, C.; Hayes, S. E.; Zhang, Y.;
617 Li, D.; Woelfel-Monsivais, C.; Sankaranarayanan, K.; McCall, L.-I. Mapping of Host-
618 Parasite-Microbiome Interactions Reveals Metabolic Determinants of Tropism and
619 Tolerance in Chagas Disease. *Science Advances*. 2020.
620 <https://doi.org/10.1126/sciadv.aaz2015>.
- 621 (43) Sumner, L. W.; Amberg, A.; Barrett, D.; Beale, M. H.; Beger, R.; Daykin, C. A.; Fan, T.
622 W.-M.; Fiehn, O.; Goodacre, R.; Griffin, J. L.; Hankemeier, T.; Hardy, N.; Harnly, J.;
623 Higashi, R.; Kopka, J.; Lane, A. N.; Lindon, J. C.; Marriott, P.; Nicholls, A. W.; Reily, M.
624 D.; Thaden, J. J.; Viant, M. R. Proposed Minimum Reporting Standards for Chemical
625 Analysis Chemical Analysis Working Group (CAWG) Metabolomics Standards Initiative
626 (MSI). *Metabolomics* **2007**, *3* (3), 211–221.
- 627 (44) *Trypanosoma Cruzi* Infection in Dogs along the US-Mexico Border: R0 Changes with
628 Vector Species Composition. *Epidemics* **2023**, *45*, 100723.
- 629 (45) Dunn, W. B.; Broadhurst, D.; Begley, P.; Zelena, E.; Francis-McIntyre, S.; Anderson, N.;
630 Brown, M.; Knowles, J. D.; Halsall, A.; Haselden, J. N.; Nicholls, A. W.; Wilson, I. D.;
631 Kell, D. B.; Goodacre, R. Procedures for Large-Scale Metabolic Profiling of Serum and

- 632 Plasma Using Gas Chromatography and Liquid Chromatography Coupled to Mass
633 Spectrometry. *Nat. Protoc.* **2011**, *6* (7), 1060–1083.
- 634 (46) Pluskal, T.; Castillo, S.; Villar-Briones, A.; Orešič, M. MZmine 2: Modular Framework for
635 Processing, Visualizing, and Analyzing Mass Spectrometry-Based Molecular Profile Data.
636 *BMC Bioinformatics* **2010**, *11* (1), 1–11.
- 637 (47) Nothias, L.-F.; Petras, D.; Schmid, R.; Dührkop, K.; Rainer, J.; Sarvepalli, A.; Protsyuk, I.;
638 Ernst, M.; Tsugawa, H.; Fleischauer, M.; Aicheler, F.; Aksenov, A. A.; Alka, O.; Allard, P.-
639 M.; Barsch, A.; Cachet, X.; Caraballo-Rodriguez, A. M.; Da Silva, R. R.; Dang, T.; Garg,
640 N.; Gauglitz, J. M.; Gurevich, A.; Isaac, G.; Jarmusch, A. K.; Kameník, Z.; Kang, K. B.;
641 Kessler, N.; Koester, I.; Korf, A.; Le Gouellec, A.; Ludwig, M.; Martin H, C.; McCall, L.-I.;
642 McSayles, J.; Meyer, S. W.; Mohimani, H.; Morsy, M.; Moyne, O.; Neumann, S.;
643 Neuweger, H.; Nguyen, N. H.; Nothias-Esposito, M.; Paolini, J.; Phelan, V. V.; Pluskal, T.;
644 Quinn, R. A.; Rogers, S.; Shrestha, B.; Tripathi, A.; van der Hooft, J. J. J.; Vargas, F.;
645 Weldon, K. C.; Witting, M.; Yang, H.; Zhang, Z.; Zubeil, F.; Kohlbacher, O.; Böcker, S.;
646 Alexandrov, T.; Bandeira, N.; Wang, M.; Dorrestein, P. C. Feature-Based Molecular
647 Networking in the GNPS Analysis Environment. *Nat. Methods* **2020**, *17* (9), 905–908.
- 648 (48) Lesani, M.; Gosmanov, C.; Paun, A.; Lewis, M. D.; McCall, L.-I. Impact of Visceral
649 Leishmaniasis on Local Organ Metabolism in Hamsters. *Metabolites* **2022**, *12* (9).
650 <https://doi.org/10.3390/metabo12090802>.
- 651 (49) Liebisch, G.; Fahy, E.; Aoki, J.; Dennis, E. A.; Durand, T.; Ejsing, C. S.; Fedorova, M.;
652 Feussner, I.; Griffiths, W. J.; Köfeler, H.; Merrill, A. H., Jr; Murphy, R. C.; O'Donnell, V.
653 B.; Oskolkova, O.; Subramaniam, S.; Wakelam, M. J. O.; Spener, F. Update on LIPID
654 MAPS Classification, Nomenclature, and Shorthand Notation for MS-Derived Lipid

655 Structures. *J. Lipid Res.* **2020**, *61* (12), 1539–1555.

656 (50) Liebisch, G.; Vizcaíno, J. A.; Köfeler, H.; Trötz Müller, M.; Griffiths, W. J.; Schmitz, G.;
657 Spener, F.; Wakelam, M. J. O. Shorthand Notation for Lipid Structures Derived from Mass
658 Spectrometry. *J. Lipid Res.* **2013**, *54* (6), 1523–1530.

659 (51) Bolyen, E.; Rideout, J. R.; Dillon, M. R.; Bokulich, N. A.; Abnet, C. C.; Al-Ghalith, G. A.;
660 Alexander, H.; Alm, E. J.; Arumugam, M.; Asnicar, F.; Bai, Y.; Bisanz, J. E.; Bittinger, K.;
661 Brejnrod, A.; Brislawn, C. J.; Brown, C. T.; Callahan, B. J.; Caraballo-Rodríguez, A. M.;
662 Chase, J.; Cope, E. K.; Da Silva, R.; Diener, C.; Dorrestein, P. C.; Douglas, G. M.; Durall,
663 D. M.; Duvallet, C.; Edwardson, C. F.; Ernst, M.; Estaki, M.; Fouquier, J.; Gauglitz, J. M.;
664 Gibbons, S. M.; Gibson, D. L.; Gonzalez, A.; Gorlick, K.; Guo, J.; Hillmann, B.; Holmes,
665 S.; Holste, H.; Huttenhower, C.; Huttley, G. A.; Janssen, S.; Jarmusch, A. K.; Jiang, L.;
666 Kaehler, B. D.; Kang, K. B.; Keefe, C. R.; Keim, P.; Kelley, S. T.; Knights, D.; Koester, I.;
667 Kosciulek, T.; Kreps, J.; Langille, M. G. I.; Lee, J.; Ley, R.; Liu, Y.-X.; Lofffield, E.;
668 Lozupone, C.; Maher, M.; Marotz, C.; Martin, B. D.; McDonald, D.; McIver, L. J.; Melnik,
669 A. V.; Metcalf, J. L.; Morgan, S. C.; Morton, J. T.; Naimey, A. T.; Navas-Molina, J. A.;
670 Nothias, L. F.; Orchanian, S. B.; Pearson, T.; Peoples, S. L.; Petras, D.; Preuss, M. L.;
671 Pruesse, E.; Rasmussen, L. B.; Rivers, A.; Robeson, M. S., 2nd; Rosenthal, P.; Segata, N.;
672 Shaffer, M.; Shiffer, A.; Sinha, R.; Song, S. J.; Spear, J. R.; Swafford, A. D.; Thompson, L.
673 R.; Torres, P. J.; Trinh, P.; Tripathi, A.; Turnbaugh, P. J.; Ul-Hasan, S.; van der Hooft, J. J.
674 J.; Vargas, F.; Vázquez-Baeza, Y.; Vogtmann, E.; von Hippel, M.; Walters, W.; Wan, Y.;
675 Wang, M.; Warren, J.; Weber, K. C.; Williamson, C. H. D.; Willis, A. D.; Xu, Z. Z.;
676 Zaneveld, J. R.; Zhang, Y.; Zhu, Q.; Knight, R.; Caporaso, J. G. Reproducible, Interactive,
677 Scalable and Extensible Microbiome Data Science Using QIIME 2. *Nat. Biotechnol.* **2019**,

678 37 (8), 852–857.

679 (52) Vázquez-Baeza, Y.; Pirrung, M.; Gonzalez, A.; Knight, R. EMPeror: A Tool for Visualizing

680 High-Throughput Microbial Community Data. *Gigascience* **2013**, 2 (1), 16.

681